

# PROCEEDINGS OF SPIE

[SPIDigitalLibrary.org/conference-proceedings-of-spie](https://SPIDigitalLibrary.org/conference-proceedings-of-spie)

## Polarization conversion on nanostructured metallic surfaces fabricated by LIPSS

A. San-Blas, N. Casquero, N. Pérez, M. Martínez-Calderon, L. Sanchez-Brea, et al.

A. San-Blas, N. Casquero, N. Pérez, M. Martínez-Calderon, L. Sanchez-Brea, J. Buencuerpo, S. M. Olaizola, A. Rodríguez, "Polarization conversion on nanostructured metallic surfaces fabricated by LIPSS," Proc. SPIE 10906, Laser-based Micro- and Nanoprocessing XIII, 109061H (22 March 2019); doi: 10.1117/12.2506982

**SPIE.**

Event: SPIE LASE, 2019, San Francisco, California, United States

# Polarization conversion on nanostructured metallic surfaces fabricated by LIPSS

<sup>a,b</sup>A. San-Blas, <sup>a,b</sup>N. Casquero, <sup>b</sup>N. Pérez, <sup>a,b</sup>M. Martínez-Calderón, <sup>c</sup>L. Sánchez-Brea,  
<sup>c</sup>J. Buencuerpo, <sup>a,b</sup>S. M. Olaizola, <sup>\*a,b</sup>A. Rodríguez<sup>a</sup>

<sup>a</sup>Ceit, Manuel Lardizabal 15, 20018 Donostia / San Sebastián, Spain

<sup>b</sup>Universidad de Navarra, Tecnun, Manuel Lardizabal 13, 20018 Donostia / San Sebastián, Spain

<sup>c</sup>Optics Department, Facultad de Ciencias Físicas, Universidad Complutense de Madrid, Ciudad Universitaria s.n., 28040, Madrid, Spain

## ABSTRACT

Waveplates modify polarization by generating a phase change. Laser Induced Periodic Surface Structures (LIPSS) have recently started to be studied as waveplates due to the birefringence induced by the nanoripples, easily fabricated in a one-step process by laser, where LIPSS morphology is defined by the characteristics of the laser process parameters and the substrate material. The optical properties of these waveplates are defined by LIPSS parameters such as period, depth or width of the ripples. In this work we have deposited thin film coatings on stainless steel samples containing LIPSS for different coating thickness and composition. Results show that thin film coatings are a good candidate for the tunability of LIPSS birefringence since the coating modifies the induced polarization change and reflectivity of the sample depending on coating thickness and composition, as expected from numerical simulations.

**Keywords:** Keywords: LIPSS, femtosecond, nanostructures, polarization, waveplate, thin-film coating

## 1. INTRODUCTION

Polarization control is a key feature in many optical setups and applications. Waveplates, the elements that transform polarization, are based on birefringence, which is present in anisotropic materials such as calcite crystals. These materials exhibit different refractive index for different axes, inducing a shift between the phases of the light in each axis, which changes its polarization. Transitive waveplates present strong dispersion [1], which is a drawback in applications involving ultrashort lasers. On the other hand, reflective waveplates prevent this issue since light is not required to travel through the element.

Nanostructured surfaces with ripples of periodicity smaller than incident light have been fabricated in recent years as reflective waveplates because the axes parallel and perpendicular to the ripples induce a change in the polarization state, thus acting as artificial birefringent materials. The properties of these waveplates are tunable through control of the parameters of the ripples such as period, depth, shape or orientation [2]. In particular, for light in the visible spectrum or in the near infrared region, ripples should be in the submicron scale. Common fabrication techniques of nanostructures with the mentioned periods include nanoimprint lithography, ultraviolet-molding or electron beam lithography.

Laser-induced periodic surface structures (LIPSS) are directional formations generated in most kinds of materials when irradiated with intense laser radiation. In recent years, LIPSS have gained interest as they present ripples with periods similar to the wavelength of the laser they are fabricated with. LIPSS fabrication is a one-step process and does not require cleanroom conditions. LIPSS have been studied in the last decades, being usually accepted that they are generated through the interaction of intense incident laser light with an electromagnetic wave scattered at the rough surface, while other models involve surface plasmon polaritons [3]. LIPSS applications include, among others, control of adhesion and migration [4], tribology [5], wetting [6] and light antireflection [7], although their use as reflective waveplates has not been well studied yet.

\* [airodriguez@ceit.es](mailto:airodriguez@ceit.es); phone 00 34 943212800; [www.ceit.es](http://www.ceit.es)

LIPSS geometry depend on the substrate material and on the laser parameters, such as: number of pulses, fluence, beam polarization or overlap [8]. However, it is difficult to fabricate LIPSS over a wide range of periods and depths with a single laser system, which may result a problem for industrial application.

Thin film coatings are layers with thickness ranging from nanometers to micrometers. They are commonly used in optics to fabricate mirrors or as reflective and antireflective coatings, controlling their properties with coating thickness and composition. Although to our knowledge dielectric coatings have never been deposited on LIPSS, they can improve their polarization changing properties and reflectivity by adding new degrees of freedom: coating thickness and composition.

Here we report the simulation and fabrication of birefringent devices consisting of dielectric coatings applied to LIPSS generated on stainless steel. Preliminary results show that induced polarization change and reflectivity can be modified with coating thickness and composition, with improvements over uncoated LIPSS, as expected from numerical simulations, showing that dielectric thin film coatings are a good candidate for the tunability of LIPSS birefringence.

## 2. MATERIAL AND METHODS

Stainless steel strips of 1 cm width, 20 cm long and 1 mm thickness were cut in a guillotine shear to pieces of 1 cm long. Prior to processing, samples were introduced in an ultrasonic bath with acetone for 5 minutes for surface cleaning purposes.

In order to fabricate LIPSS, a Ti:Sa (titanium-doped sapphire) laser with pulses of 130 fs, central emitting wavelength at 800 nm and repetition rate of 1 kHz was used. Maximum pulse energy available is 3 mJ. An attenuator composed of a half wave plate in combination with a polarizing beam splitter was used to control the energy delivered to the sample, and a neutral density filter further decreased the energy to 1  $\mu$ J. The laser beam was directed onto the sample through a 10x microscope objective (Fig. 1). The sample was moved under the laser irradiation describing parallel lines of width 10  $\mu$ m each until an area of 3x3 mm<sup>2</sup> was filled. The polarization of the laser radiation was controlled with another half wave plate so that the orientation of the LIPSS can be adjusted. Experiments were carried out in open air atmosphere. After processing, samples were again cleaned for 5 minutes in an ultrasonic bath with acetone.

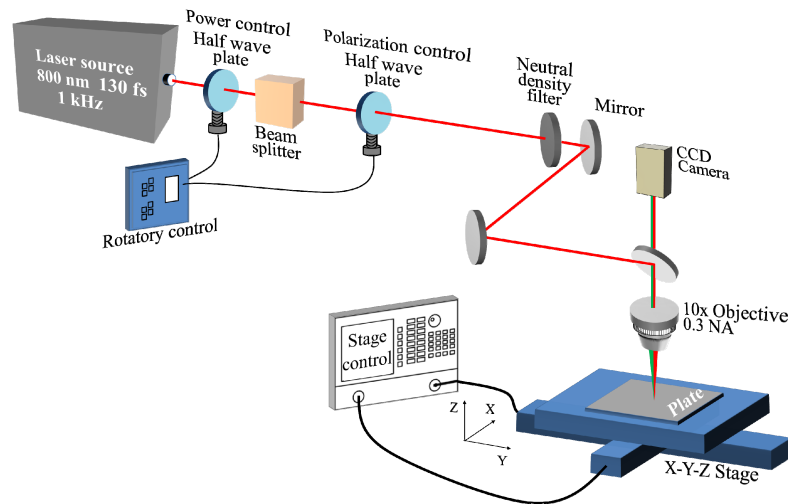


Fig. 1. Schematic diagram of the laser processing station.

Plasma Enhanced Chemical Vapor Deposition (PE-CVD) was used to create the thin films. SiO<sub>2</sub> was deposited on four samples with different thicknesses of 50, 100, 200 and 300 nm, and Si<sub>3</sub>N<sub>4</sub> was deposited on another four samples with the same four thicknesses. An additional sample was left uncoated for comparison.

A Scanning Electron Microscope (SEM) was used to analyze the surface topography of the irradiated samples. The open source software Gwyddion was used to perform two dimensional Fast Fourier Transforms (2D-FFT) of the SEM micrographs, which provides an effective way to analyze the LIPSS period and orientation, as well as the Dispersion of the LIPSS Orientation Angle (DLOA).

Images of the transversal profile of LIPSS and coatings were obtained with the technique Focused Ion Beam (FIB), incorporated in the same microscope along with SEM. FIB uses focused ions which eliminates part of the surface of the sample, so that it is possible to obtain a transversal cut. In order to do this, the sample was tilted  $52^\circ$  (Fig. 2). Before the FIB technique is to be applied a platinum nanometric layer is deposited on the sample, in order to protect the surface, so that the ions only penetrate from the side.

Changes in polarization induced by the samples were determined with a commercial polarimeter (Thorlabs PAX1000IR1). HeNe (633 nm wavelength) and 808 nm diode continuous lasers were used. Reflectivity was measured using a supercontinuum laser (NKT superk compact), acquiring the reflected light with an integrating sphere connected to a spectrometer.

### 3. NUMERICAL SIMULATIONS

In our simulations we have tested three scenarios of sample configuration: LIPSS with no coating (Fig. 2-left), LIPSS with SiO<sub>2</sub> uniform coating (Fig. 2-center) and LIPSS with SiO<sub>2</sub> conformal coating (Fig. 2-right). For all of them, the input was an 850 nm wavelength laser with linear polarization at  $45^\circ$  with respect to the LIPSS orientation, and LIPSS period is 580 nm.

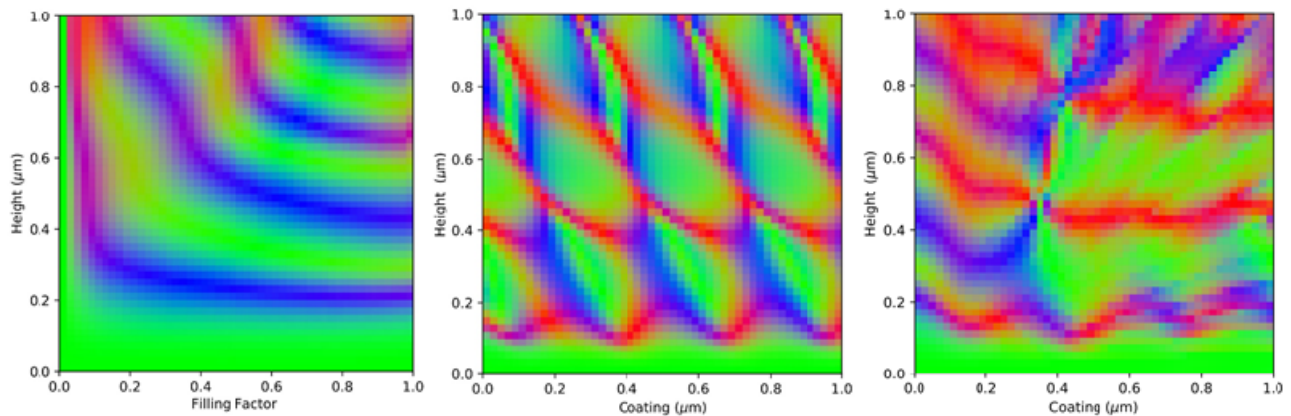


**Fig. 2** [left] Q (red) U (green) V (blue) Stokes parameters of the reflected beam from uncoated LIPSS. For the input  $45^\circ$  linearly polarized wave, green means no change, red means change to  $0^\circ$  linear polarization, and blue means change to circular polarization. X-axis indicates the relative width of the ripples. [center] FDTD simulation for LIPSS with SiO<sub>2</sub> coating, the coating being uniform, this is, having constant height with respect to the horizontal plane. In this scenario, X-axis represents the coating thickness [right] FDTD simulation for LIPSS with SiO<sub>2</sub> conformal coating. This means that coating thickness is constant along the profile of the LIPSS.

Results show that polarization can be changed for certain parameters. In the first scenario, where LIPSS are present without coating, there is only change for certain heights, while filling factor is not determining. Also, changes in polarization can only be seen for changes in height of around  $200 \mu\text{m}$ , which is difficult to achieve without changing the laser source. In the scenarios with coating, the pattern observed in the simulations is different, with variations also depending on the coating thickness. In addition, varying coating thickness with precision and in a wide range of thicknesses is plausible for most deposition techniques.

#### 4. FABRICATION AND POLARIZING BEHAVIOUR OF NON-COATED SUBWAVELENGTH GRATINGS

Single lines were written in the SS plates with a variable scan speed,  $v$ , from  $0.1$  to  $1 \text{ mm}\cdot\text{s}^{-1}$ . The corresponding effective number of pulses per beam spot,  $N$ , is calculated as  $N=2\omega f/v$ , being  $f$  the repetition rate (1kHz) and  $\omega$  the beam spot size. The beam spot is defocused in order to adjust the peak fluence,  $F$ , to  $1.04 \text{ J}\cdot\text{cm}^{-2}$ , near the ablation threshold. SEM micrographs revealed the presence of LIPSS perpendicularly oriented to the laser beam polarization for all the tested conditions.

In order to analyze the average period of the LIPSS,  $\Lambda$ , as a function of the number of pulses, two-dimensional fast Fourier transform (2D-FFT) were obtained from SEM micrographs. Fig. 2 shows that the period of the LIPSS slightly decreases from 630 to 580 nm as the number of pulses increases, corresponding with LSFL. For a number of pulses over 50 two different periods of the LIPSS are obtained: the 2D-FFT revealed an additional periodicity between 325 and 350 nm, corresponding to HSFL.

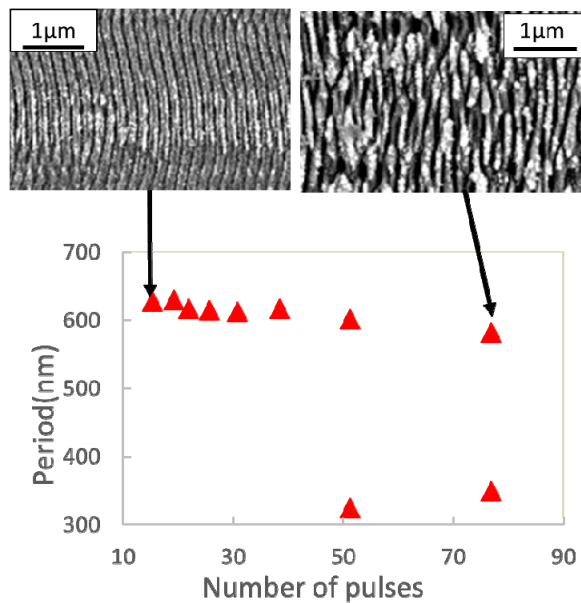


**Fig. 3.** Evolution of the LIPSS period as a function of the number of applied pulses for LSFL (left) and HSFL (right).

To measure the depth of the LIPSS, the processed SS plates were cut via FIB; Fig. 4 shows that the LIPSS depth grows as the number of pulses increases; this rise of depth is, approximately, linear when the number of pulses is under 50. Analogously to the LIPSS period, when the number of pulses was over 50, two different depths were measured (see Fig. 3). The deepest LIPSS are related to LSFL and the shallowest groves to HSFL.

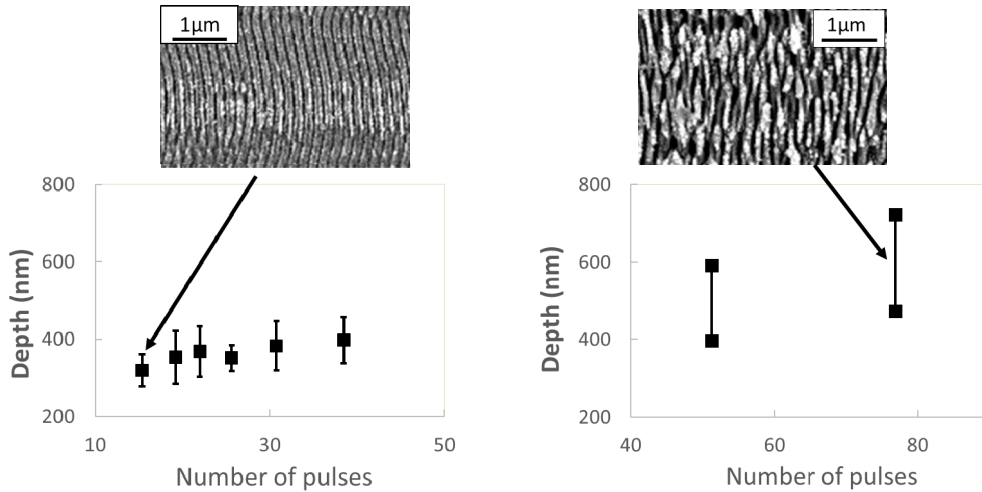


**Fig. 4.** Evolution of the LIPSS depth as a function of the number of applied pulses for LSFL (left) and LSFL/HSFL (right).

In order to fabricate large area sub-wavelength reflective gratings (period 580 and 630 nm), the conditions that provided LIPSS with the best quality were selected. Although LSFL generally appear perpendicularly oriented to the beam polarization vector, their homogeneity greatly depends on the orientation of the electric field vector with respect to the sample scanning direction. Therefore, large-area gratings were fabricated for different polarization directions, as shown in Fig. 5.

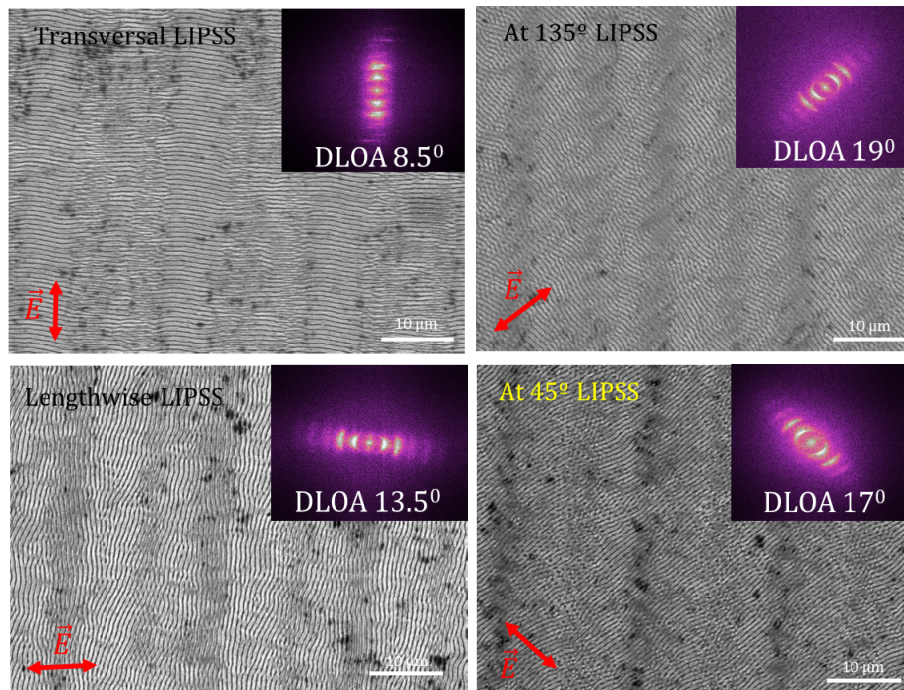


**Fig. 5.** Large area gratings fabricated with different orientation and their corresponding 2D-FFT (insets) and DLOA.

As expected, LSFL perpendicularly oriented to the beam polarization were obtained in all the cases. However, different values were obtained for the DLOA, as can be seen in Fig. 4; LIPSS are more homogeneously oriented for a scanning direction linearly or perpendicularly aligned to the polarization direction.

The results of the previous study were used to determine the optimal parameters for obtaining 580 nm sub-wavelength gratings with homogeneously oriented LIPSS. The capability of these gratings to convert light polarization states was analyzed and the main results are presented in Fig. 6.

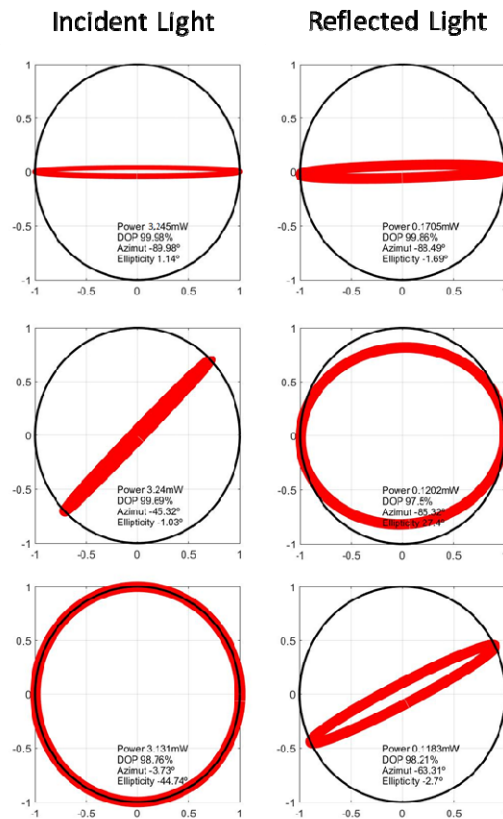


**Fig. 6** Polarization behavior of LIPSS gratings. (left) Incident light on LIPSS covered surface and (right) reflected light from LIPSS covered surfaces.

As expected from simulations, when these gratings were interrogated with linearly polarized light aligned with the LIPSS orientation direction, no polarization change was observed in the reflected beam. On the other hand, when interrogated with linearly polarized light at an angle of 45° with respect to the LIPSS orientation direction, circularly polarized light is obtained. Analogously, when impinged with circularly polarized light, linearly polarized light with an ellipticity lower than 2.70 is obtained in the reflected beam. These results confirm the existence of form birefringence in the LIPSS processed surfaces. This is, to the best of our knowledge, the first report on the use of LIPSS for polarization conversion.

## 5. CHARACTERIZATION AND POLARIZING BEHAVIOUR OF COATED SUBWAVELENGTH GRATINGS

Images obtained after the FIB procedure (Fig. 7) show profiles where the coatings have a very conformal configuration, which is relevant information for numerical simulations. LIPSS depth is irregular, but a statistical analysis reports an average depth of 340 nm.

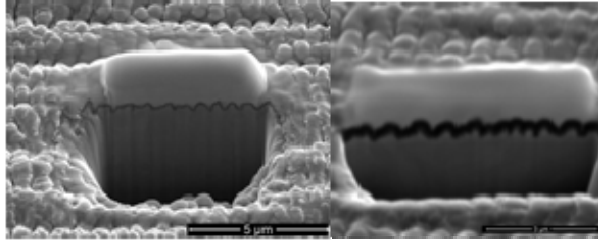


**Fig. 7** Images obtained after using the FIB technique. A transverse section of the LIPSS (dark grey) with coating over it (black) can be seen. The amorphous material over the coating (light grey) is the platinum used in the FIB procedure. Left:  $\text{SiO}_2$  coating of thickness 50 nm. Right:  $\text{Si}_3\text{N}_4$  coating of thickness 300 nm.

Results obtained in the polarization change show that for certain coating thicknesses and materials, the change in polarization induced differs greatly from one sample to another (Fig. 8), as predicted by numerical simulations. However, they do not show a trivial relation with coating thickness and material. Results are also sensitive to the wavelength of the laser used. These results show that it is possible to tune the response of LIPSS without varying their parameters by adding a dielectric coating.

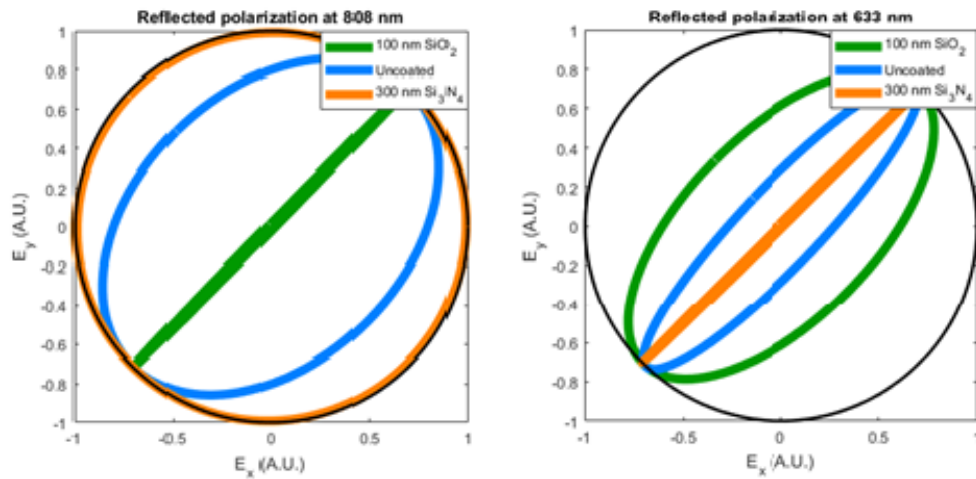


**Fig. 8.** Polarization state of the reflected beam for three samples with different coatings. Laser wavelength used is 808 nm (top) and 633 nm (bottom). Incident polarization is  $45^\circ$ . Under certain conditions some samples introduce ellipticity, differing from the response of the uncoated sample.

Variations of the reflective properties of LIPSS have been observed in the coated samples (Fig. 9). Thin film coatings modify LIPSS reflectivity in certain regions of the spectrum which, depending on composition, thickness, and wavelength, can improve the reflectivity of the uncoated sample. Since high reflectivity is desirable for applications where low energy loss is expected, this is an optical property to be held into account along with the potential for polarization change.



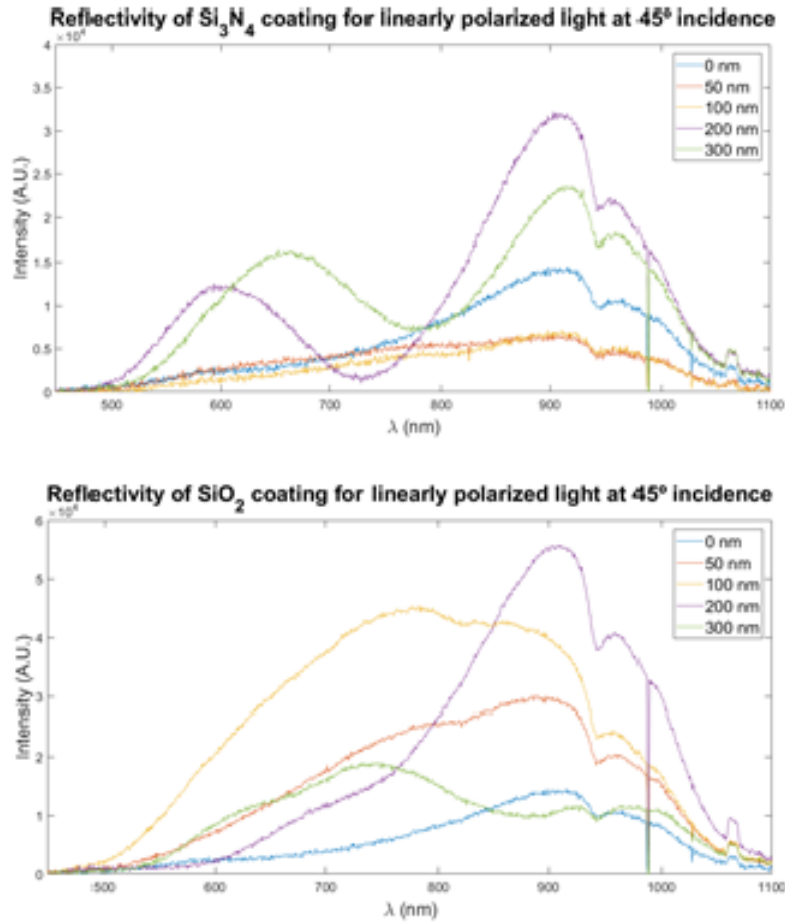


Fig 9 Reflected spectra obtained for coated and uncoated samples for the two materials used in the deposition: silicon nitride (top) and silicon dioxide (bottom). Higher intensity at certain wavelengths can be seen for some of the samples with coating than that for the uncoated sample (blue line).

## CONCLUSIONS

Gratings fabricated via LIPSS are able to convert the incident linear polarized laser light at 633 nm into reflected circular polarized light, and vice versa, with ellipticity values lower than  $2.7^\circ$ . This fabrication approach can enable low cost fabrication of subwavelength diffraction gratings for polarization conversion.

In the light of the obtained results, we can conclude that dielectric thin film coatings are a good candidate for the tunability of LIPSS birefringence, with reflectivity being an important factor that can also be improved by the coating.

Another important result is that, in the range of studied thicknesses, the coating geometry is conformal. This will be considered in further simulations, where LIPSS irregularity should also be accounted for.

## ACKNOWLEDGEMENTS

This work is part of the following projects: ECOGRAB, funded by the Government of Spain under the RETOS COLABORACIÓN I+D+i programme. LASER4SURF has received funding from the European Union's Horizon 2020 research and innovation programme under grant agreement No 768636.

## REFERENCES

- [1] N. Passilly, P. Karvinen, K. Ventola, P. Laakkonen, J. Turunen, and J. Tervo, *J. Eur. Opt. Soc.*, vol. 3, 2008.
- [2] S. S. Stafeev, V. V. Kotlyar, A. G. Nalimov, M. V. Ko-tlyar, and L. O'Faolain, *Photonics Nanostructures - Fundam. Appl.*, vol. 27, pp. 32–41, 2017.
- [3] J. Bonse, S. Höhm, S. Kirner, A. Rosenfeld, and J. Krüger, *Conference on Lasers and Electro-Optics*, 2016, vol. 23, no. 3, p. STh1Q.3.
- [4] M. Martínez-Calderon et al., *Sci. Rep.*, vol. 6, no. July, p. 36296, 2016.
- [5] J. Bonse et al., *Appl. Surf. Sci.*, vol. 336, pp. 21–27, May 2015.
- [6] M. Martínez-Calderon, A. Rodríguez, A. Dias-Ponte, M. C. Morant-Miñana, M. Gómez-Aranzadi, and S. M. Olaizola, *Appl. Surf. Sci.*, 2016.
- [7] A. Y. Vorobyev and C. Guo, *Opt. Express*, vol. 19 Suppl 5, pp. A1031-6, Sep. 2011.
- [8] S. Gräf and F. A. Müller, *Appl. Surf. Sci.*, vol. 331, pp. 150–155, Mar. 2015.